Journal of Statistical Physics, Vol. 63, Nos. 5/6, 1991

Fermion Nodes

D. M. Ceperley[1]

Received January 4, 1991

The knowledge of the nodes of the many-fermion wave function would enable exact calculation of the properties of fermion systems by Monte Carlo methods. It is proved that fermion nodal regions have a tiling property, there is only one distinct kind of nodal region. All others are related to it by permutational symmetry. For some free particle systems, it is shown that there are only two nodal regions. An explicit form for the nodes of the many-fermion density matrix would enable exact simulations to be carried out at finite temperature. In the high-temperature limit, its nodes are related to Voronoi polyhedra. Two-dimensional cross sections of nodes are depicted. General computable families of fermion wave functions and density matrices are discussed.

KEY WORDS: Nodes; fermions; density matrix; simulations of quantum systems.

1. INTRODUCTION

In this paper I investigate general features of the nodes of many-body fermion wave functions and density matrices. There seems to be surprisingly little published about this subject even though the one-dimensional case is often presented in introductory textbooks on quantum mechanics. This problem is interesting because of its relationship to the calculation of the thermodynamic properties of many-fermion systems, one of the outstanding problems in computational physics.

A rigorous and practical simulation method for many-fermion systems is not yet known. The problem can be stated as follows. Does there exist a method to calculate properties (say the energy) of a fermion system to a given (sufficiently small) accuracy in a computer time which grows as a power of the number of fermions? Naturally, no uncontrolled approxima-

[1] National Center for Supercomputing Applications, Beckman Institute, Department of Physics, University of Illinois at Urbana-Champaign, Champaign, Illinois 61820.

822/63/5-6-28

tions are allowed, so that error bounds represent true errors on the exact energy. Ideally one would like to perform such a calculation at any temperature or for any excitation level. In the high-temperature limit, quantum systems reduce to classical ones, and the only methods which can determine properties of classical many-body systems are stochastic: molecular dynamics and Monte Carlo methods. By extension, one expects the corresponding quantum methods at a lower temperature will be stochastic.

The first approach that I consider here, Green's function Monte Carlo[2,3,16] (also known as diffusion Monte Carlo or projector Monte Carlo), takes an initial trial function and projects out the ground state as

$$\phi = \lim_{t \to \infty} \exp(-t\mathscr{H})\Psi_T \tag{1}$$

where $\mathscr{H}$ is the Hamiltonian. The thermal evolution operator $\exp(-t\mathscr{H})$ can be interpreted as a diffusion and branching process, if the wave function is interpreted as a probability density, but unless one is in the absolute (boson) ground state, the wave function changes sign and thus cannot be treated directly as a probability density. This is the origin of the sign problem in the simulation of quantum systems. Naive methods of solving the sign problem take an exponential amount of computer time to achieve high accuracy,[21] exponential in the number of degrees of freedom. While practical methods have been found for specific small systems, simulations of large systems will always be necessary for studying physical systems which contain several length scales, such as those undergoing phase transitions.

A useful and powerful approximation is the fixed-node approximation,[16] where one assumes knowledge of where the exact wave function is positive and negative. Let $\Psi_T(R)$ be a trial wave function. Then one assumes that

$$\phi(R) = 0 \qquad \text{if} \quad \Psi_T(R) = 0 \tag{2}$$

Then the diffusion equation implicit in Eq. (1) is solved by simulating the diffusion process within the domains bounded by the assumed fixed nodes. Condition (2) is satisfied if the random walks are constructed not to cross the nodes of the trial wave function.

This fixed-node method has many desirable features. If the nodes are correct, then the method is exact. The algorithm only needs to know when the system crosses a node; nothing else about the wave function is required. The method yields the best possible upper bound to the energy consistent with the assumed nodes.[4] This implies that the energy is second order in

the displacement of the assumed nodes from the exact nodes. It has been found that the upper bound produced by this approximation is often excellent.[3,6] The method calculates properties in a polynomial time since for large systems, the computer time will be dominated by the time taken to determine whether the system has crossed a node. Typically, one chooses nodes from a Slater determinant. Finding the numerical value of a general determinant requires order N^3 operations. Thus, knowledge of the nodes implies the ability to simulate the thermodynamic properties of a fermion system in polynomial time.

As good as the fixed-node method is, it does not satisfy our criteria for solving the fermion problem unless one knows that the assumed nodes are exact (or sufficiently close to exact, since one can perturb around them with the release-node method[6]). This is our principal motivation for summarizing the little that is known about fermion nodes. I will first describe the ground-state situation and show some nodes of these systems. Then I will make the generalization to nonzero temperature. I will then prove that some noninteracting fermion systems have maximally connected nodal cells. I will discuss general procedures for constructing accurate and computable antisymmetric functions. These results are new and may be of some help in solving the many-fermion problem.

2. THE NODES OF THE GROUND STATE

For simplicity I will always discuss a system of N electrons in the absence of a magnetic field. They could just as easily be N ^{3}He atoms. Nucleons with their spin and momentum-dependent forces are significantly more complicated. I will only discuss the continuum, time-independent Schrödinger equation:

$$\mathscr{H}\phi(R) = -\lambda\nabla^2\phi(R) + V(R)\,\phi(R) = E_0\phi(R) \tag{3}$$

where $R = \{\mathbf{r}_1, \mathbf{r}_2, ..., \mathbf{r}_N\}$ is the set of electron coordinates, $V(R)$ is the total potential energy, and $\lambda = \hbar^2/2m$. In this paper I am almost always concerned with general potentials, particularly the Coulomb interaction between charged particles, and I will usually assume it is the sum of one-body and two-body potentials,

$$V(R) = \sum_{i=1}^{N} v_1(\mathbf{r}_i) + \sum_{i<j} v_2(\mathbf{r}_i, \mathbf{r}_j) \tag{4}$$

Frequently I will assume that the potential is finite almost everywhere. Replacing the Coulomb potential with a finite one for very small intercharge separations will not change the type of nodal properties to be

discussed. By free particles, I mean systems for which the potential vanishes.

Particles obeying Fermi statistics are antisymmetric with respect to the exchange of both spin and spatial coordinates:

$$\phi(PR, P\Sigma) = (-1)^P \phi(R, \Sigma) \tag{5}$$

where the $\Sigma = (\sigma_1, ..., \sigma_N)$ are discrete spin variables equal to $\pm\hbar/2$ and P is an arbitrary permutation, and $(-1)^P$ refers to the sign of the permutation. For the above Hamiltonian, which does not flip spins, it is permissible to fix the spin variables and impose antisymmetry only with respect to interchanges between coordinates of electrons with the same spin. That is, spatial antisymmetry is only required for permutations that satisfy

$$P\Sigma = \Sigma \tag{6}$$

Spatial antisymmetry only applies to electrons of the same spin. The z component of the spin angular momentum is thus fixed to be $(\hbar/2)(N_\uparrow - N_\downarrow)$. I will *always* assume Eq. (6) holds. Factoring the wave function like this can complicate the analysis of rotational symmetry, but is not known to cause problems in extended many-body systems. Let me also introduce the antisymmetrization projection operator:

$$\mathcal{A}f(R) = \sum_P \frac{(-1)^P}{N_P} f(PR) \tag{7}$$

where $N_P = N_\uparrow! \, N_\downarrow!$ is the total number of allowed permutations.

The node of the wave function, $\phi(R)$, in the set of points where $\phi(R) = 0$. In the absence of a magnetic field, the wave function can be assumed to be real, since both the real and imaginary parts of the wave function separately satisfy the Schrödinger equation. If the ground state is nondegenerate, then the two parts must be proportional to each other, so their nodes must be at the same location. I will discuss the degenerate case below. The total configuration space is a Cartesian manifold of dimension dN, where d is the spatial dimensionality, always 1, 2, or 3 in this paper. For a real function, a single equation specifies the nodes so they will have dimension $dn - 1$.

What properties do the nodes have? First of all, the *coincidence planes* $\mathbf{r}_i = \mathbf{r}_j$ are located on the nodes, where $\mathbf{r}_i$ and $\mathbf{r}_j$ are two particles with the same spin. These are hyperplanes of dimension $dN - d$. For electrons in one dimension ($d = 1$), the dimensionality of the coincidence planes equals the dimensionality of the nodal planes, so it is at least possible that these

special planes exhaust the nodes. That is often the case in one dimension, as will be shown below. In one dimension, exchange only occurs by particles passing through each other.[15] Since there are $N!$ ways of ordering N particles on a line, one sees that there must be at least $N!$ nodal regions in one dimension. Periodic boundary conditions reduce this number to $(N-1)!$. In the next section, I will prove that there cannot be more, which proves that the nodal surfaces are equivalent to two particles occupying the same point, a fact which is well known. In more than one dimension these coincidence planes are only a scaffolding through which the nodes pass. There is much greater flexibility of the nodal surfaces in higher dimensions and they are not usually fixed by general arguments.[14]

Clearly, the nodes must possess all the symmetries of the ground-state wave function, at least in the nondegenerate case. For example, if the Hamiltonian is translationally invariant, then the nodes must have translational invariance. This is only a d-dimensional restriction on the nodes, so it does not greatly constrain them.

Let me correct a common misconception. I am discussing in this paper the nodes of the exact many-body wave function. These are very different from the nodes of one-body orbitals. Let us take the Ne atom with ten electrons as an example. It has $1s$, $2s$, and $2p$ fully occupied orbitals. These orbitals have various spatial nodes: i.e., the $2s$ function has a radial node and the $2p$ orbitals have planar nodes going through the origin. These nodes have next to nothing to do with the many-body nodes, which are a 29-dimensional manifold located in the 30-dimensional space of the electron coordinates.

Consider the rectangle shown in Fig. 1, and assume the potential has inverse symmetry about its center: $V(\mathbf{r}) = V(-\mathbf{r})$. States which are antisym-

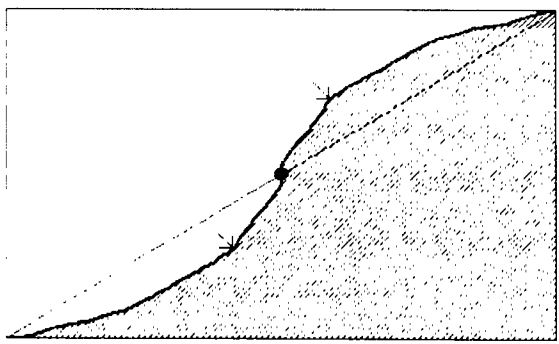

Fig. 1. The potential in the rectangle has inversion symmetry about its center, the black dot. Shown are two possible nodes for the first odd-parity state. A fixed-node solution solves the Schrödinger equation everywhere, but the gradient of the solution will not match at points related by symmetry, e.g., the two points shown with arrows.

metric about the center are analogous to fermion states. Clearly the center is a point (dimension 0) on the nodal line (dimension 1). The curve itself has inversion symmetry, so the portion on the right half is related to the portion on the left half. The tiling property discussed next implies that there are always exactly two nodal regions, no matter how complicated the potential is. But without specifying the potential everywhere, I do not know how the nodal line will bisect the rectangle. As mentioned earlier, the fixed-node method consists of making an ansatz for the nodal line (such as the diagonal line shown) and solving the Schrödinger equation with that assumption. It yields an upper bound, but, in general, not the exact solution, because the gradient of the solution does not match at points related by symmetry, e.g., the two points shown with arrows.

It may happen that the ground state is degenerate. This implies that the nodal surface is arbitrary to some extent. A simple example is two free 1D particles in periodic boundary conditions (on a circle). For convenience suppose the box has length 2π. Then the single-particle orbitals are proportional to 1, e^{-ix}, and e^{ix}. The two-particle ground state is twofold degenerate, since one can occupy either the positive or negative momentum state. All the real antisymmetric many-body ground states can be written in the form $\cos(x_1-\theta)-\cos(x_2-\theta)$ for θ an arbitrary phase. The nodes of the wave function are $x_1=x_2$ and $x_1+x_2=2\theta$ and are shown in Fig. 2. One of the nodes is fixed by symmetry, while the other depends on an arbitrary phase. The second node is not translationally invariant. We cannot keep translational symmetry and work with real functions for degenerate systems. The point $x_1=x_2=\theta$ is a critical nodal point where

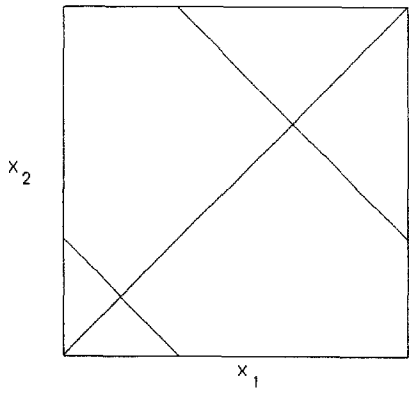

Fig. 2. The nodes of two free 1D particles in periodic boundary conditions are given by the equations $x_1=x_2$ and $x_1+x_2=2\theta$. The point $x_1=x_2=\theta$ is a critical nodal point where the two nodes cross and the wave function vanishes quadratically.

the two node cross, necessarily at a right angles (independent of the potential) and the wave function vanishes quadratically.

Suppose a general energy level is p-fold degenerate. We can always pick $p-1$ independent many-body coordinates (points) and find a linear transformation such that all the transformed wave functions vanish at all but one of those points. Therefore degeneracy always implies some freedom in the choice of the nodes. In the above example, we can specify one point on the second node.

In a few special cases,[14] such as the $^3S_1$ triplet ground state of the He atom ($1s2s$), the nodal surfaces are determined by the other symmetries of the problem. Since it is rotationally symmetric, the wave function can be expanded in powers of the three interparticle distances: r_1, r_2, and r_{12}. Antisymmetry then implies that the sphere $r_1 = r_2$ is the exact nodal set.

Shown in Fig. 3 is a 2D cross section of the ground-state wave function of 161 free (polarized) fermions in a 2D square box. This system has a unique, nondegenerate ground state. Naturally, I cannot hope to show much of the complexity of this 322-dimensional function, so what I have

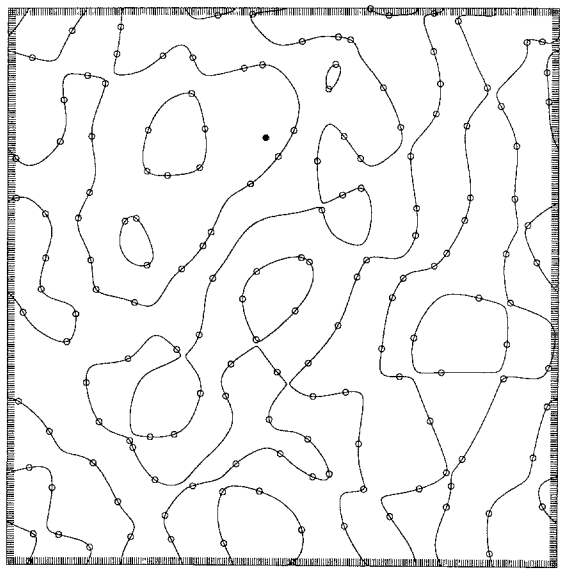

Fig. 3. A 2D cross section of the ground-state wave function of 161 free (polarized) fermions in a periodic square. All 161 particle positions were sampled using variational Monte Carlo from $\phi(R)^2$. The filled circle indicates the original position of the first particle. The other 160 particles are fixed at positions indicated by the open circles, and nodes of the wave function as a function of the position of the first particle are plotted. The resolution of the contouring program is approximately half of the fine scale shown around the border of the plot.

done is to fix 160 particles at a typical (random) position, indicated by the open circles, and plotted the nodes of the first particle. In fact, all 161 particle positions were sampled using variational Monte Carlo from $\phi(R)^2$. The filled circle indicates the original position of the first particle. The shortest length scale in the wave function is that of the Fermi wavelength, which is π times the interparticle spacing. Since the nodes pass through the positions of the fixed particles, the fermion wave function gives a unique procedure for connecting the open circles with lines. By examining the picture, one can see that the nodal regions are almost connected in the cross section. There are only a few isolated pockets which do not connect with the rest of the positive or negative regions. It is not surprising that if one allows some of the fixed particles to move, the entire positive or negative portion of the wave function is fully connected. I will demonstrate later in the paper that free particle systems have *maximal nodal cells*; there is a single positive and negative nodal cell. Another feature that is apparent in this cross section are the many places where it appears as if the nodes are crossing, or about to cross. These are places where the nodes are parallel to this cross section.

2.1. The Tiling Property

Define a *nodal cell* $\Omega(R)$ around a point R as the set of all points which can be reached from R without crossing a node. R is assumed not to be on a node: $\phi(R) \neq 0$. If the potential is reasonable, the ground-state nodal cells have the tiling property: any point R' not on the node is related by symmetry to a point in $\Omega(R)$, i.e., there exists a permutation P such that $R' = PR''$, where $R'' \in \Omega(R)$. In other words, $\sum_P \Omega(PR)$ equals entire space minus the nodal set. There is only one type of nodal cell; all other cells are simply copies obtained by relabeling the particles. Applied to Figs. 1 and 2, this implies that there can be most two nodal regions. The tiling property is the generalization to fermions of the theorem that a bosonic ground state is nodeless.

The proof of the tiling property is quite simple and is based on the fact that the absolute or bosonic ground state is nodeless and has a *lower* energy than the first excited state. Assume, to the contrary, that the tiling property does not hold for the antisymmetric eigenfunction $\phi(R)$ with energy E. Then $\sum_P \Omega(PR)$ leaves out some nodal cells and there must exist two distinct nodal cells $\Omega(R_1)$ and $\Omega(R_2)$ which have a common border and are not related to each other by a permutation. In that case one can construct a lower energy fermion wave function by eliminating the node between the two cells. This will be possible if the potential is local and reasonable, meaning that it is not infinite everywhere along the node

separating the two cells. Then there will exist another function, ϕ', defined and positive in $\Omega(R_1) \cup \Omega(R_2)$ and zero outside, with $\mathscr{H}\phi' = E'\phi'$ and lower energy $E' < E$, since eliminating a node always lowers the energy. A properly antisymmetric function defined in the whole space is obtained by using the antisymmetrization projection operator: $\tilde{\phi}'(R) = \mathscr{A}\phi'(R)$. This extended wave function is strictly positive in $\Omega(R_1) \cup \Omega(R_2)$, since otherwise $\Omega(R_1)$ and $\Omega(R_2)$ would have been related by a permutation. Hence $\tilde{\phi}'(R)$ can be normalized and has a variational energy:

$$E_0 \leqslant \frac{\int dR\, \tilde{\phi}'(R)\, \mathscr{H}\tilde{\phi}'(R)}{\int dR\, \|\tilde{\phi}'(R)\|^2} = E' < E \tag{8}$$

Hence, I have constructed an upper bound to the ground-state energy lower than that of the starting wave function, which proves that the nodes of $\phi(R)$ could not have corresponded to the ground-state nodes.

Pair potentials will always be reasonable in the sense defined above since they are only infinite at the coincident planes which are of dimension $dN - d$ and cannot separate two nodal cells for $d > 1$. A one-body potential with some electrons in one box and some electrons in another box and an infinite potential between is not reasonable since putting nodes in the space between the boxes will not cost energy. One might try to construct the following counterexample to the tiling property. Find any antisymmetric function without the tiling property. It is the solution to the Schrödinger equation with a potential $\nabla^2\phi/\phi$. The tiling property implies that either this potential is not reasonable because $\nabla^2\phi$ does not vanish when $\phi(R)$ does, or that there exist lower energy eigenstates than $\phi(R)$.

There are two implications of the tiling property for fixed-node Monte Carlo. First, one should try and prove that one's favorite functions have the tiling property. In some cases that is very easy. If the wave function is the exact solution to some model problem with a reasonable potential, then it will satisfy this condition. For example, wave functions coming from the solution to a mean field equation like the local density functional approximation are satisfactory. It is possible (though unlikely) that Hartree–Fock solutions will not have the tiling property, since they are derived from a nonlocal potential and locality was implicitly used in the proof. (For example, nonlocal potentials can be constructed which have as a bosonic ground state a wave function with nodes.) Second, for approved functions, variational and fixed-node random walks can safely remain inside one nodal cell and never have to worry about sampling the other side, since phase space is identical on the other side. This property does not tell us how many nodal cells there are, but only gives an upper bound of N_P.

The above proof of the tiling property is valid whether or not the ground state is degenerate. Thus, all of the states in a degenerate subspace will have the tiling property. One can generalize this result for the case where there are other discrete symmetries present. Suppose one wants the lowest antisymmetric state with odd parity under the inversion operator $\tilde{R}$. Then the ground state will have the tiling property with respect to the combined action of P and $\tilde{R}$.

2.2. Average Distance to the Nodes

In a high-dimensional space it is difficult to visualize the character of the nodes. The momentum distribution $n(k)$ gives a rough feeling for the nodal spacing. The single-particle off-diagonal density matrix[20] is defined as

$$n(\mathbf{r}) = \int dR\, \phi^*(\mathbf{r}_1, \mathbf{r}_2, \ldots, \mathbf{r}_N)\, \phi(\mathbf{r}_1 + \mathbf{r}, \mathbf{r}_2, \ldots, \mathbf{r}_N) \tag{9}$$

In a variational Monte Carlo calculation,[17] $n(r)$ is computed from Eq. (9) by sampling a configuration from $\phi(R)^2$, then displacing a single particle a distance r and averaging the ratio of the wave function at the new position to the wave function at the original position:

$$n(\mathbf{r}) = \left\langle \frac{\phi(\mathbf{r}_1 + \mathbf{r}, \mathbf{r}_2, \ldots, \mathbf{r}_N)}{\phi(\mathbf{r}_1, \mathbf{r}_2, \ldots, \mathbf{r}_N)} \right\rangle \tag{10}$$

The Fourier transform of the single, particle density matrix gives the momentum distribution:

$$n_k = \frac{1}{(2\pi)^3} \int d\mathbf{r}\, e^{-ik\cdot\mathbf{r}} n(\mathbf{r}) \tag{11}$$

For free particles, the momentum distribution is a step function with only momentum states less than the Fermi wave vector k_F filled. Then Eq. (11) implies that the single-particle density matrix $n(\mathbf{r})$ is a Bessel function $(k_F r)^{d/2} J_{d/2}(k_F r)$, where d is the dimensionality. This function oscillates with its first zero occurring at $k_F r = (3.14, 3.83, 4.49)$ in one, two, and three dimensions, respectively. The value of this zero tells us when on the average a displaced particle is as likely to be on one side of the node as the other. The averaging is with respect to the full wave function. The fact that this function becomes positive at larger r means that there is a long-range periodicity in the free particle nodes. The single-particle density matrix decays algebraically like $r^{-(d+1)/2}$ in any system that has a discontinuity at

some value of momentum. Thus, the long-range nodal structure has something to do with physical observables. Consider averaging the square of the ratio of the displaced wave function in Eq. (10). One finds

$$\left\langle \left[\frac{\phi(\mathbf{r}_1 + \mathbf{r}, \mathbf{r}_2, \ldots, \mathbf{r}_N)}{\phi(\mathbf{r}_1, \mathbf{r}_2, \ldots, \mathbf{r}_N)} \right]^2 \right\rangle = 1 \tag{12}$$

It is the sign of the wave function which causes $n(\mathbf{r})$ to decay, not its magnitude.

If two particles are displaced in Eq. (9), that defines the two-particle off-diagonal density matrix and its Fourier transform is the two-particle momentum distribution. This distribution is related to Cooper pairs and superconductivity. Liquid helium is a good example of how displacing two electrons can give quite different results than moving one. If a whole He atom is displaced in such a way that it does not overlap with other atoms, no nodes are crossed and the wave function appears bosonlike.

2.3. Critical Points on the Nodal Surface

A nodal surface is locally a hyperplane almost everywhere. However, it is possible for nodal surfaces to intersect. A little though about how one would define node crossing in a high-dimensional space shows that crossing will occur at *critical* points R where one has both $\phi(R) = 0$ and $\nabla\phi(R) = 0$. These are saddle points on the nodes. It is possible, of course, that there are no such critical points, since the definition encompasses $dN + 1$ conditions.

Let us do a Taylor expansion of $\phi(R)$ about a critical point R, assuming the potential is finite nearby and that the second derivative matrix, the Hessian, does not vanish. The Laplacian of $\phi(R)$ must vanish at R since $\phi(R)$ is a solution of Schrödinger's equation and the potential is finite, which implies that the sum of the eigenvalues of the Hessian matrix must vanish. Of the dN eigenvalues, say there are $m > 0$ negative eigenvalues and $0 < n \leqslant dN - m$ positive eigenvalues. The wave function near R will be of the form $\sum_{i=1}^{n+m} a_i x_i^2$ and the nodes a conical quadric hypersurface.

If there are only two nonzero eigenvalues, the positive eigenvalue must equal the magnitude of the negative eigenvalue and the nodes will cross at right angles. For three nonzero eigenvalues, the nodal surface will be like the familiar light cone in relativity. For four nonzero eigenvalues the nodal surface is either the light cone (three positive eigenvalues and one negative one) or a hyperboloid which turns into a cone.

The dimensionality of the critical nodal point equals the number of zero eigenvalues. Some zero eigenvalues can be supplied by translational or rotational degrees of freedom. Locally there will always be only two nodal

cells coming together at the critical point if $m > 1$ and $n > 1$. If the Hessian matrix vanishes, even more complicated situations can arise. In two dimensions, if the first nonvanishing derivative at the critical point is order n, then n nodal lines come together,[19] separated by equal angles of π/n.

It is easy to find one critical point on the free particle nodal surface. Simply place the fermions on a perfect Bravais lattice in periodic boundary conditions. I find that the free particle wave function vanishes like $\phi(R) = (R - Z)^\chi$, where χ is an exponent roughly proportional to the total number of fermions and Z is a perfect lattice; see Fig. 4 for the behavior of the exponent versus the number of fermions in a square box. A pair potential would normally have a global minimum for some Bravais lattice. Thus, the critical point is in precisely the wrong location to minimize the potential energy. The precise value of the dimension of the critical point presumably depends on the symmetry group for that particular number of particles. A practical consequence of the existence of this critical point is that a random walk should not be started too near a perfect lattice configuration.

2.4. Possible Antisymmetric Functions

Although I have made little progress in stating exact conditions that nodes must obey, there remains the further problem in a fixed-node quantum Monte Carlo simulation of determining if a node is crossed for a

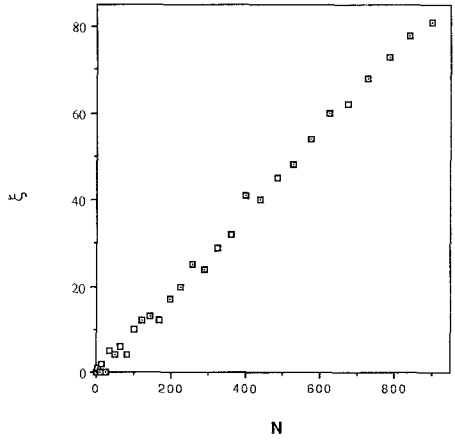

Fig. 4. The exponent giving the behavior of the particle wave function for N (polarized) fermions in a periodic square as the coordinates approach a square lattice. The exponents are all integers. In the case where the ground state is degenerate only one of the wave functions was checked.

given antisymmetrical trial function in a reasonable amount of computer time. Here nature and mathematics work to our advantage since it is possible to compute the values of determinant in N^3 operations. The corresponding function for bosons, a permanent, can only be computed in computer time proportional to $N!$, so it is necessary in simulations of bosons to directly sample the permutations. A determinant and a related object, a Pfaffian, are all that have been used for a many-fermion simulation. In this section I will assume that the system is unpolarized, so that the number of spin-up electrons equals the number of spin-down electrons:

$$I = N_\uparrow = N_\downarrow \tag{13}$$

The simplest and most commonly used many-body wave function is the pair-product or Bijl–Jastrow–Slater function[2]:

$$\Psi_1(R) = \exp\left[-\sum_{i<j} u(r_{ij})\right] \|\varphi_i(\mathbf{r}_j^\uparrow)\| \, \|\varphi_i(\mathbf{r}_j^\downarrow)\| \tag{14}$$

where $u(r)$ is a pair correlation function and $\varphi_i(\mathbf{r})$ is a set of I orbitals. $\|\cdots\|$ indicates the determinant of the matrix. Both the u and $\varphi_i(\mathbf{r})$ are determined variationally or from another theoretical calculation. If the orbitals are determined from the exact solution to a local one-body problem, then the nodes will have the tiling property. It is evident that the factor $u(r)$ will not affect the nodes, since it is real.

Finding the value of a general determinant takes I^3 operations. Free particles in one dimension are described by a Vandermonde determinant, which requires only I^2 operations. In fact, to find the sign in one-dimension is even faster (for a local move) since one only need to count the number of pair interchanges. There exist wave functions with unusual Fermi surface in two and three dimensions which can be done faster than I^3 operations, but it is not known whether these methods can be made general. Insulating systems have orbitals which decay exponentially fast and evaluation of the resulting determinant can be speeded up with the use of sparse matrix algorithms.

What general way is there of improving the nodes of the Slater determinant? In quantum chemistry it is standard to use an expansion in a basis of Slater determinants. The optimal basis to expand is composed of eigenfunctions of the single-particle dcensity matrix, the natural orbitals. However, an expansion in single-particle functions converges very slowly, simply because the number of possible excitations grows exponentially with the number of degrees of freedom. If there is a degeneracy or near degeneracy in the ground state that is broken by interparticle correlation it is very important to keep multiple determinants. In general, however, we

want to look for nonperturbative ways to increase the accuracy of the nodes.

One of the successes of recent years has been the understanding of the structure of the wave function of a strongly correlated quantum Fermi liquid, namely liquid ^{3}He. Good agreement for the total binding energy was obtained when backflow effects were put into the Slater determinant[4] in Eq. (11). The original idea was suggested by Feynman and Cohen[12] based on conservation of particle current and the variational principle. I will sketch a general method of improving wave functions based on stochastic averages or path integrals.

Given any trial function $\Psi_n(R)$, one can improve it by projecting it with the Hamiltonian as in Eq. (1). Define the local energy as $E_n(R) = \Psi_n(R)^{-1} \mathscr{H} \Psi_n(R)$. If the trial function were exact, the local energy would be a constant. Let us define a random walk process by the diffusion and drift equation (the Smoluchowski equation):

$$-\frac{df(R,t)}{dt} = \lambda \sum_{i=1}^{N} \nabla[-\nabla f(R,t) + 2f(R,t)\nabla \ln(\Psi_n(R))] \tag{15}$$

Then, in terms of this stochastic process one can write[5,18] the projected wave function with a generalized Feynman–Kac formula:

$$\Psi_{n+1}(R) = e^{-\mathscr{H}\tau}\Psi_n = \Psi_n(R)\left\langle \exp\left[-\int_0^\tau dt\, E_n(R(t))\right]\right\rangle_{DRW} \tag{16}$$

where $\langle \cdots \rangle_{DRW}$ means averaging with respect to the stochastic process defined in Eq. (15) and beginning (or ending) at the point R. Note that antisymmetrization, being linear, will commute with the averaging operations, so I will start with the unsymmetrical version of the pair product trial function:

$$\Psi_1(R) = \exp\left[-\sum_{i<j} u(r_{ij})\right] \prod_{i=1}^{N} \varphi_i(\mathbf{r}_i) \tag{17}$$

Then the local energy is

$$E_1(R) = W(R) - \lambda \sum_{i=1}^{N} [2\nabla_i \ln \varphi_i(\mathbf{r}_i)\nabla_i U + (\nabla_i U)^2] \tag{18}$$

where $W(R)$ is a sum of one- and two-body functions and $U(R)$ is the total pair-correlation factor. In general it is impossible to evaluate analytically the averages over the random walk. Here I make a crude approximation of correcting the trial function by the local energy itself, but optimize

functions that appear in it to partially account for the stochastic averaging. Then the improved fermion trial function will have the form

$$\Psi_2 = \mathscr{A}\Psi_1(R)\exp[-\tau\tilde{E}_1(R)]$$
$$= \exp\left[-\sum_{i<j} u(r_{ij}) + \sum_{i=1}^{N} (\nabla_i U)^2\right] \|M_{ij}^{\uparrow}\| \, \|M_{ij}^{\downarrow}\| \tag{19}$$

with the new matrix

$$M_{ij} = \varphi_i(r_j)\exp[\nabla_j \ln \varphi_i(\mathbf{r}_j)\cdot\nabla_j \tilde{U}] \tag{20}$$

There are two new terms in $\Psi_2(R)$; backflow, which is the correction inside the determinant and which affects the nodes, and a three-body bosonlike correction[22] which does not affect the nodes. Taking the case of free particles in periodic boundary conditions where the single-particle orbitals are plane waves $\exp(i\mathbf{k}\cdot\mathbf{r})$, we see that instead of working with the bare coordinates $\mathbf{r}_i$, one should consider the dressed "quasiparticle" coordinates:

$$\mathbf{x}_i = \mathbf{r}_i + \nabla_i \tilde{U}(R) \tag{21}$$

where $\tilde{U}(R)$ is some effective potential, symmetric with respect to allowed permutations, to be optimized.

This can be considered as a general procedure of mapping from real coordinates to some kind of quasiparticle coordinates, then using a simple one-body wave function of the quasiparticle coordinates. It is not known whether the exact wave function can be written in this form for a reasonable $\tilde{U}$ and what are the conditions that it must satisfy to give the tiling property.

Another kind of antisymmetric function is derived from BCS theory for singlet pairing or equivalently by multiplying the two matrices in Eq. (14) together:

$$\Psi_{1s}(R) = \left\{\exp\left[-\sum_{i<j} u(r_{ij})\right]\right\} \|\chi_s(\mathbf{r}_j^{\uparrow}, \mathbf{r}_k^{\downarrow})\| \tag{22}$$

where I have assumed the system has the same number of up and down electrons, and $\chi(\mathbf{r}, \mathbf{s})$ is the symmetric s-like pairing function:

$$\chi_s(\mathbf{r}, \mathbf{s}) = \sum_{i=1}^{I} \varphi_i(\mathbf{r})\,\varphi_i(\mathbf{s}) \tag{23}$$

Recently[8] a generalization of the BCS-type function for triplet pairing has been proposed. A Pfaffian is defined[13] as the antisymmetric product of pair functions:

$$P(\mathbf{r}_1, \mathbf{r}_2, \ldots, \mathbf{r}_N) = \frac{(I!)^2}{2^I}\mathscr{A}\prod_{i=1}^{I} \chi_p(\mathbf{r}_{2i}, \mathbf{r}_{2i-1}) \tag{24}$$

where $\chi_p(\mathbf{r}, \mathbf{s})$ is an antisymmetric pairing function and electrons 1 through I are up and $I+1$ through N are down. It is not obvious that this function will be computable, because the effect of the antisymmetrization is to generate an exponential number of terms. However, the square of a Pfaffian is

$$P(R)^2 = \|\chi_p(\mathbf{r}_j^{\downarrow}, \mathbf{r}_k^{\downarrow})\| \, \|\chi_p(\mathbf{r}_j^{\uparrow}, \mathbf{r}_k^{\uparrow})\| \tag{25}$$

so it is possible to compute the magnitude of a Pfaffian in order I^3 operations. But fixed-node calculations require the sign as well and there does not seem to be a simple way to calculate the sign of the Pfaffian. This is not a fundamental problem, since it is not hard to establish whether in a given move from R to R' the determinant has vanished in between. One simply has to search for the minimum on a given path and show that the minimum is not zero. Good wave functions must be smooth to have low kinetic energy, so it should be easy to find the minimum.

3. THE NODES OF THE DENSITY MATRIX

3.1. The Fixed-Node Finite-Temperature Method

The properties of fermion systems at positive temperature are arguably even more important than those of the ground state. After all, physical systems are constrained to be at nonzero temperature and most phase transitions occur at finite temperature. The *thermal fermion problem* is the construction of a polynomial-time algorithm for the computation of the exact thermodynamics of a many-fermion system at positive temperature. The complexity of the algorithm should be a power of both the size of the system and the inverse temperature. I will now describe a generalization of the fixed-node method which could solve this problem if only the nodes of the fermion density matrix were known.

At nonzero temperatures one wants to calculate properties with respect to the many-body density matrix:

$$\rho_F(R, R_0; \beta) = \sum_{\alpha} e^{-\beta E_\alpha} \phi_\alpha^*(R) \, \phi_\alpha(R_0) \tag{26}$$

where the sum is over the complete set of antisymmetric eigenfunctions of $\mathscr{H}$ and $\beta = 1/k_B T$. The density matrix can be expanded in terms of path integrals to give

$$\rho_F(R_0, R_0; \beta) = \mathscr{A} \int dR_1 \cdots dR_{M-1} \prod_{i=1}^{M} \rho(R_{i-1}, R_i; \tau) \tag{27}$$

where $\tau = \beta/M$, the boundary conditions are $R_M = R_0$, and $\rho(R_{i-1}, R_i; \tau)$ are distinguishable particle density matrices. For them the sum in Eq. (26) is over all eigenfunctions irrespective of symmetry. Antisymmetry is put in by the antisymmetric projection operator, which allows the paths to close on themselves as $R_M = PR_0$, where P is a permutation, and a sign $(-1)^P$ is associated with this walk. The density matrix is expanded into a path since accurate expressions exist for the density matrix as τ becomes small. But at low temperature, the straightforward use of Eq. (27) to simulate a fermion system becomes exponentially inefficient because the contribution from positive permutations approximately equals the contribution from negative permutations. Thus, a fermion estimator becomes exponentially small with respect to the noise. The computer time needed to achieve a given accuracy on a fermion observable will be exponential in the number of electrons and in $\beta = 1/k_B T$.

Let us reformulate antisymmetry in terms of a boundary condition. The fermion density matrix can also be defined as the solution to the Bloch equation

$$\frac{d\rho_F(R, R_0; \beta)}{d\beta} = -\mathscr{H}\rho_F(R, R_0; \beta) \tag{28}$$

with the initial conditions

$$\rho_F(R, R_0; 0) = \mathscr{A}\delta(R - R_0) \tag{29}$$

In what follows I will denote the second argument of the density matrix R_0 as the *reference point* and the set of points $\{R_t\}$ for which there exists a continuous "space-time" path with $\rho_F(R_{t'}, R_0; t') > 0$ for $0 \leqslant t' \leqslant t$ the *reach* of R_0, or $\Upsilon(R_0, t)$.

Suppose that the reach is known in advance. It is a simple matter (see Appendix C) to show that the problematical initial condition, Eq. (29), can be replaced by a zero boundary condition on the surface of the reach. It follows because the fermion density matrix is a unique solution to the Bloch equation (28) with the zero boundary conditions.

Now, one can find a path integral solution without the minus signs. One simply restricts the paths in Eq. (27) to lie in $\Upsilon(R_0, t)$. I will call these the fixed-node paths. If one averages over the distribution of reference points, one can obtain all diagonal fermion observables. Hence the nodes of $\rho_F(R, R_0; t)$ are of great interest. *If I could compute the sign of the fermion density matrix in polynomial time, the thermal fermion simulation problem would be solved.* The fixed-node path integral Monte Carlo method consists in using the nodes of a good estimate of $\rho_F(R, R_0; t)$, called the trial density matrix, to restrict the paths. If its nodes are substantially

correct, the method can calculate exact thermodynamics of the fermion system at any temperature.

Again let me warn the reader that the nodes of the density matrix are quite different from excited-state nodes of the Schrödinger equation. It is thought that the nodes in highly excited states are very complicated, especially when the corresponding classical system is chaotic. But in thermal equilibrium, it is precisely in the high-temperature (classical) limit that things simplify.

The nodes of the fermion density matrix are somewhat more complicated than those of the ground-state wave function, since $\rho_F(R_t, R_0; t)$ depends on $2dN+1$ variables. In what follows I will usually take R_0 and t to be fixed. With these variables fixed, the nodes are a $dN-1$ manifold in a dN-dimensional space, just as in the ground state, and I can speak of nodal cells. Note that the density matrix is always real, and, in contrast to the wave function, it is always uniquely defined. At large times the nodes will converge to the ground-state nodes if the ground state is nondegenerate.

The density matrix has the following general symmetry properties:

$$\rho_F(R, R_0; t) = \rho_F(R_0, R; t) = (-1)^P \rho_F(PR, R_0; t) \tag{30}$$

The coincidence planes $\mathbf{r}_i = \mathbf{r}_j$ are on the nodes for all R_0 and t. The reference point itself is not a node, since

$$\rho_F(R_0, R_0; t) > 0 \tag{31}$$

unless all wave functions vanish at R_0. I will always assume *the potential at the reference point is finite and the reference point is not a coincidence plane or on a ground-state node.* We have translation invariance only if both R and R_0 are simultaneously translated, because of the initial conditions of Eq. (29).

Define a nodal cell $\Omega(R, R_0, t)$ as the set of points $\{R_1\}$ that can be reached from R by a path at constant R_0 and t with a nonvanishing density matrix. If the ground state is nondegenerate, this will reduce to our previous definition at low temperature (t large). We have previously defined the reach, $\Upsilon(R_0, t)$. Let me repeat the distinction between a nodal cell and the reach. Nocal cells are connected by nonzero paths at a fixed time, while the reach is defined as those points R connected to the reference point by a positive path beginning at $(R_0, 0)$ and ending at (R, t). The reach is the relevant domain for fixed-node paths at finite temperature. One of the interesting open questions is the condition that these two domains be equal.

Clearly $R_0 \in \Upsilon(R_0, t)$, since the trivial path $R_t = R_0$ has a positive density matrix. Also, $\Omega(R_0, R_0, t) \subseteq \Upsilon(R_0, t)$. It is shown in Appendix C

that the reach has the tiling property for all t. That is, every point with a nonzero value of the fermion density matrix can be reached by a strictly positive or strictly negative path starting from one of the copies of the reference point.

A volume, such as the nodal cell or the reach, is said to be *maximal* if it bisects all space. All the positive regions are then interconnected. Symmetry implies the negative regions would also be interconnected. The argument in Appendix C implies that if the reach is maximal for some time t, it is maximal at all larger times.

3.2. The Free Particle Fermion Density Matrix

The free particle density matrix has the form

$$\rho_0(R, R_0; t) = (4\pi\lambda t)^{-dN/2} \left\| \exp\left[-\frac{(r_i - r_{j0})^2}{4\lambda t} \right] \right\| \tag{32}$$

assuming the boundaries are far away. Explicit forms for alternative boundary conditions or for free particles in an external potential will have the Gaussians replaced with the appropriate single-particle density matrices.

Then the nodal surface for two free particles in an infinite spaces is given by the hyperplane

$$(\mathbf{r}_1 - \mathbf{r}_2) \cdot (\mathbf{r}_{10} - \mathbf{r}_{20}) = 0 \tag{33}$$

The FN path must stay in a half-plane (in relative coordinates) defined by the reference point R_0 as shown in Fig. 5, independent of the temperature.

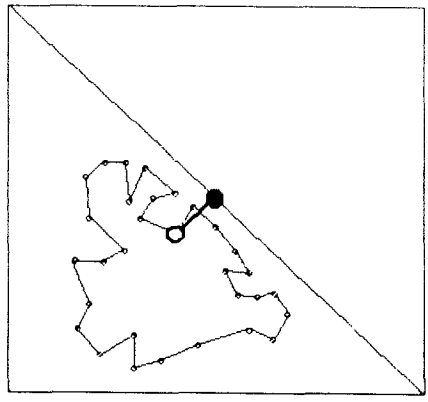

Fig. 5. The phase space allowed for paths of two free particles. Plotted is the path in relative coordinates. The large open circle is the reference point. The large filled circle is the coincident plane. The fixed-node path must keep to the left of the indicated line as given by Eq. (33).

Since there is a degeneracy in the ground state with periodic boundary conditions, the nodal surface always depends on R_0 as well as R. Rotational symmetry is restored only by averaging with respect to the reference point.

The situation for three free particles is more complex, since it is possible for them to rotate without crossing a node. For example, if the reference point consists of an equilateral triangle, a rotation about the center of the triangle by an arbitrary angle will not cross a node. It is shown in Appendix A that if the reference point is an acute triangle (all three angles less than 90°) the rotation will never cross a node in the high-temperature limit.

See Figs. 6 and 7 for a cross section of the nodes of the free particle density matrix for 161 particles in two dimensions at a temperature range of $2.5 \leqslant T/E_F \leqslant 10$ (Fig. 6) and $0.04 \leqslant T/E_F \leqslant 0.025$ (Fig. 7). Here E_F is the Fermi energy and equals $4\pi\lambda\rho$, where $\rho = n/A$ is the particle density. The ground state is nondegenerate and has an excitation energy to the first excited state of $0.039E_F$. Figure 6 is well into the classical regime, while Fig. 7 is approaching, but has not reached the ground-state contours of Fig. 2. The reference point in this figure coincides with the cross section of the ground-state wave function of Fig. 2. At the smallest value of β one can quite clearly see the approach to the limiting, piecewise linear form of the

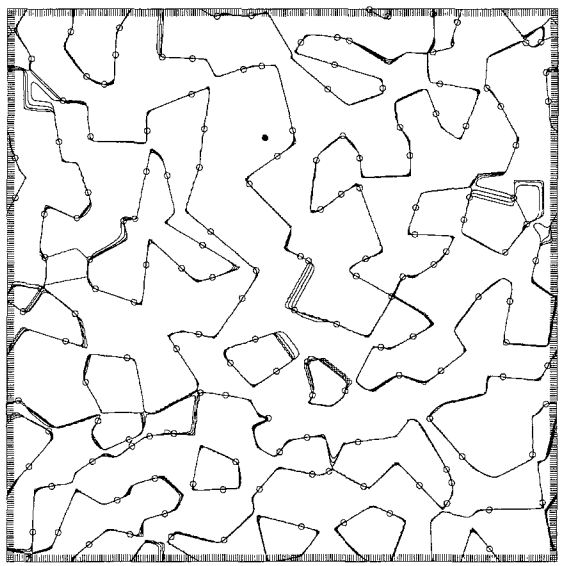

Fig. 6. The reference point and symbols are identical to Fig. 2. These are contours of the nodes of the free particle density matrix for $2.5 \leqslant T/E_F \leqslant 10$, where E_F is the Fermi energy.

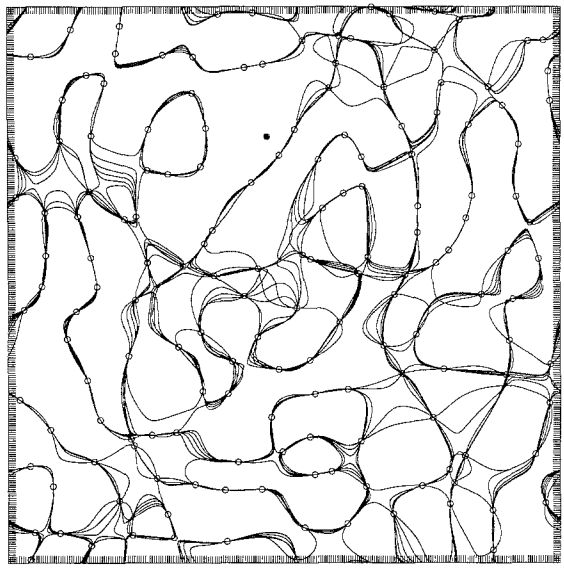

Fig. 7. The reference point and symbols are identical to Fig. 2. These are contours of the nodes of the free particle density matrix at $0.04 \leqslant T/E_F \leqslant 0.25$. The energy of the first excited state is $0.039E_F$ above the ground state, so these nodes are approaching those of Fig. 2.

nodes to be discussed below. Even with the pinning of the coincident planes the nodes evolve substantially in going from high to low temperature.

3.3. The Classical Limit

The nodes of the density matrix have an especially simple form in the high-temperature limit regardless of the potential. First define a *permutational cell* $\Delta_P(R_0)$ as the set of all points closer to PR_0 than to any other $P'R_0$. These are Voronoi, Dirichlet, or Wigner–Seitz polyhedra—convex polyhedra bounded by hyperplanes $R \cdot (PR_0 - P'R_0) = 0$. Note that there are exactly N_P of these cells and that all are essentially the same.

Their relationship to the free particle nodal cells is easy to derive at high temperature. Expand the free particle determinant of Eq. (32) in terms of permutations. For a point R inside the region $\Delta_P(R_0)$, the permutation P will dominate the expansion as t goes to zero, since, by definition, the distance to PR_0 is smallest, and all the other terms are exponentially damped relative to it. Thus, $\rho_F(R, R_0; 0)$ will have the sign of P inside $\Delta_P(R_0)$. The nodal cells of $\rho_F(R, R_0; 0)$ consist of the permutational cells $\Delta_P(R_0)$ with the following important modification. If two permutational

cells with the same sign share a common face, then there is no node separating them and those two permutational cells belong to the same nodal cell. If the same-sign nodal cells share enough interfaces, then the positive nodal cells can percolate through the entire positive volume and the nodal cells will be maximal.

Let us now show that the nodes for any system with a bounded potential reduce to free particle nodes in the high-temperature limit. The Feynman–Kac[10] formula for the density matrix is

$$\rho_F(R, R_0; \beta) = \mathscr{A}\rho_0(R, R_0; \beta) \left\langle \exp\left[-\int_0^\beta dt\, V(R(t)) \right] \right\rangle \tag{34}$$

where $\langle \cdots \rangle$ means the average over all Brownian paths connecting R with R_0, and ρ_0 is the free particle (distinguishable-particle) density matrix. Let us assume the potential energy is bounded: $|V(R)| < V_0$ for all R. (This is much stronger than I need.) Then clearly each term in the permutational sum implied by $\mathscr{A}$ approaches the free particle term. As β goes to zero, at a fixed value of R and R_0, the interacting fermion density matrix will approach the free fermion density matrix. Then it is clear that the exponential terms for the kinetic energy dominate and for any bounded potential, the nodes of the exact interacting density matrix equal the nodes of the free particle density matrix as $\beta \to 0$.

In the high-temperature limit, the nodal cell of R_0 is the same as the reach of R_0, since the definition of the permutational cell does not involve t, but only distances:

$$\Omega(R_0, R_0, 0) = \Upsilon(R_0, 0) \tag{35}$$

The critical points are places where $\nabla\rho_F(R, R_0; \beta)$ and $\rho_F(R, R_0; \beta)$ vanish. Nodal surfaces can only cross at a critical point. Assume the density matrix is critical at R^* and β^*, and the potential is bounded near the critical point. Expanding it in the neighborhood and using Eq. (28) gives to lowest order

$$\rho_F(R, R_0; \beta) \approx (\beta - \beta^*)\,\mathrm{Tr}(\bar{\gamma}) + (R - R^*)\,\bar{\gamma}(R - R^*) \tag{36}$$

where $\bar{\gamma}$ is a symmetric tensor of size dN by dN. If $\bar{\gamma}$ has only positive or only negative eigenvalues, the nodal surfaces will be like a finger that ends at β^*. Otherwise the critical point describes crossing of nodes with lines along the principle axes of $\bar{\gamma}$ which are connected for $\beta > \beta^*$, disconnected $\beta < \beta^*$, and vice versa. As the system approaches the ground state, there can be no time dependence in the nodes and we recover $\mathrm{Tr}(\bar{\gamma}) = 0$.

3.4. Forms of the Trial Density Matrix

A neon atom is a good example of the sort of problems one encounters in constructing a trial density matrix which smoothly goes from the free particle form, correct at high temperature, to the spherically symmetric-like Hartree–Fock nodes. Actually this is easy to treat. Simply solve for the single-particle density matrix in the "self-consistent" field of the nucleus and the other nine electrons, $v_{\text{eff}}(\mathbf{r})$. Then the equation for the one-body orbitals is

$$-\frac{d\phi(\mathbf{r}, \mathbf{r}_0; t)}{dt} = [-\lambda \nabla^2 + v_{\text{eff}}(\mathbf{r})]\, \phi(\mathbf{r}, \mathbf{r}_0; t) \tag{37}$$

with boundary condition

$$\phi(\mathbf{r}, \mathbf{r}_0; 0) = \delta^3(\mathbf{r} - \mathbf{r}_0) \tag{38}$$

The trial density matrix should also contain interactions between electrons, similar to the pair-product term in ground-state trial functions:

$$\rho_1(R, R_0; t) = \exp[-U(R; t) - U(R_0; t)]\, \mathscr{A} \prod_{i=1}^{N} \phi(\mathbf{r}_i, \mathbf{r}_{i0}; t) \tag{39}$$

Clearly for $v_{\text{eff}} = 0$ this gives the free particle nodes and will go over to the Hartree–Fock-like trial function at low temperature. The anti-symmetrization converts the product into a determinant as in Eq. (32). Numerically it will be essential to keep the various orbitals orthogonal at low temperature.

One can include backflow effects in several different ways and it is not yet clear which is superior. First of all, one can use the local-energy method described in Section 2.4 to find corrections to the above density matrix:

$$\rho_1(R, R_0; t) = \exp[-U(R; t) - U(R_0; t)]\, \mathscr{A} \prod_{i=1}^{N} \phi(\mathbf{r}_i + \mathbf{F}_i, \mathbf{r}_{i0} + \mathbf{F}_{i0}; t) \tag{40}$$

where $\mathbf{F}_i \approx (t^2\lambda/2)\, \nabla_i V(R)$ is proportional to the classical force. This will be correct at small t.

To motivate another form, think of the density matrix that would be needed in a hydrogen plasma, with fast-moving electrons and slow-moving, but not static, protons. Then one might wish to use an instantaneous effective potential such as

$$v_{\text{eff}}(\mathbf{r}; R, R_0) = \frac{1}{2} \sum_{i=1}^{N} \bar{u}(\mathbf{r} - \mathbf{r}_i) + \bar{u}(\mathbf{r} - \mathbf{r}_{i0}) \tag{41}$$

where $\bar{u}(\mathbf{r})$ is some smeared-out potential function. The mass of the electron appearing in Eq. (37) (inside λ) should become a temperature-dependent effective mass. If the effective potential becomes attractive between unlike spins, in principle, one could obtain S-wave BCS functions at low temperatures.

4. THE MAXIMAL PROPERTY OF FREE PARTICLE NODAL CELLS

In this section I show that the free particle density matrix breaks the configuration space into a single positive and negative region. I examined all free particle systems in two and three dimensions in a periodic square or cube for $N \leqslant 200$. In all cases I have proven with a computer construction of paths that those free particle node cells are maximal. I have not shown that arbitrary fermion systems are maximal, though the high-temperature results prove that the reach of most systems is likely maximal.

To find an upper bound to the number of nodal cells, I first pick a reference point R_0. For simplicity assume the density matrix or wave function is positive there. Then I examine the straight-line (constant-time) path connecting R_0 to $p_{ijk}R_0$ to find whether the global minimum along this path is negative. At high temperature I know that the straight-line path is optimal, but at low temperatures (or in the ground state) one may wish to deform the path to find a strictly positive path. Since density matrices and (wave functions) are relatively smooth (otherwise they would have high kinetic energy), it is not computationally difficult to find the minimum. If I do find a positive minimum, the three electrons (ijk) are then said to be connected and assigned to the same cluster. When all nearest neighbor triangles have been examined, the resulting clusters (containing $n_1, n_2, \ldots, n_c$ particles each) give us an upper bound $2^c N!/(n_1!\, n_2! \cdots n_c!)$ to the number of nodal cells.

If there is only one cluster containing all the up electrons and a cluster containing all the down electrons, then this proves the nodal cells are maximal. The tiling property guarantees that the bound is independent of the choice of reference point. However, for some reference points, the paths will be easier to locate and the resulting upper bound lower. The algorithm will give the exact number of nodal cells only if all even permutations and all deformations of the paths are examined. Since each point along the path takes order N^2 operations to perform and there are $O(N)$ nearest neighbor triangles to examine, the algorithm is order N^3.

I have numerically computed the nodes for two types of systems, free particles in a two- or three-dimensional box, and particles in a filled band of a periodic potential. In all cases only a single cluster was found. Thus the

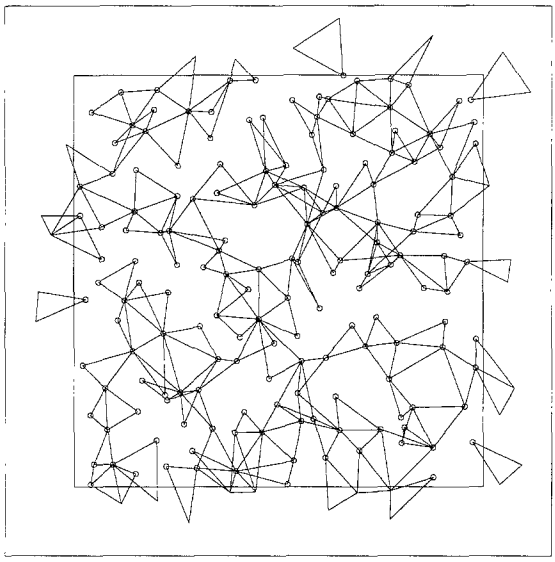

Fig. 8. Allowed fixed-node triplet permutations in the high-temperature limit for the reference point of Fig. 2. Particles may be connected also by the periodic boundary conditions which are given by the inner square. All the triangles form a single cluster and the nodal cell for 161 particles in a square is maximal.

upper-bound algorithm works well. For my choice of R_0, I always found many triangles were feasible; see Fig. 8 as an example of the cluster construction. In the case of degenerate ground states I only examined a single member of the ground-state manifold.

The second set of calculations was for 121 particles in an external potential given by $q[\cos(2x)+\cos(2y)]$. I had originally thought that an insulator would show radically different nodal patterns than a crystal, but I was mistaken and the patterns are rather similar. The low-temperature nodal cells are maximal for this insulator. But the many-body wave functions for an insulator are exponentially localized.

5. CONCLUDING REMARKS

In boson systems it is the presence of macroscopic permutations which is responsible for superfluidity[1] and long-range order. It is interesting to speculate that the same could hold for fermion systems. Liquid ^{3}He becomes superfluid in the temperature range 1–2 mK, depending on density. There are two distinct superfluid phases at zero magnetic field, the A and B phases. This transition temperature is three orders of magnitude lower than the superfluid transition temperature for liquid ^{4}He (boson).

Since the fixed-node method is exact given the correct nodes, this phase transition must manifest itself in some way. For example, perhaps the transition is similar to the one in ^{4}He where long permutation cycles become probable at the transition temperature. Superfluidity would occur at a much lower temperature for fermions because of a bottleneck in configuration space caused by the nodes of the density matrix. It is not at all obvious how the p-wave order parameters (in the A and B phases) emerge from this description.

We are in the process of carrying out simulations of liquid ^{3}He based on the fixed-node path integral algorithm. If the turning on of permutations is involved in the superfluid transition of fermion liquids, this would provide a radically different view of fermion superfluidity and would unify the theoretical description of helium liquids.

As is evident, very little is really known about the exact properties of the nodes in fermion systems. Much more work is needed along the lines I have tried to sketch in this paper. All the programs described in the text are available upon request. The author would appreciate any comments and corrections. Email address: ceperley@ncsa.uiuc.edu.

APPENDIX A. CONDITIONS FOR CLASSICAL EXCHANGE

Here I calculate whether two permutational cells are connected in the high-temperature limit in free space, i.e., there are not periodic boundary conditions. Let R_0 be the reference point. As discussed in Section 3.3, the condition that the nodal cell around R_0 be connected to that around $P_0 R_0$, where P_0 is an even permutation, is that there exists a path from R_0 to $P_0 R_0$ for which the distance to an even permutation is always smaller than the distance to an odd permutation.

Let us first consider the situation for just three particles. It is clear that the above condition reduces to the following: the three even regions will be connected iff the following straight-line path always remains closer to an even point than to an odd point:

$$\|\lambda(P_0 R_0 - R_0)\| < \|R_0 + \lambda(P_0 R_0 - R_0) - P_1 R_0\| \tag{A1}$$

where $0 < \lambda < 1/2$ and P_0 ranges over the even permutations and P_1 ranges over the odd permutations. By expanding out the distances, regrouping, and taking the worst case of $\lambda = 1/2$, one arrives at the condition

$$\Delta_1(\Delta_1 - \Delta_0) > 0 \tag{A2}$$

where

$$\Delta_i = P_i R_0 - R_0 \tag{A3}$$

is a $3N$-dimensional vector. For three particles we only need to check the two triplet permutations against the three pair permutations. Without loss of generality take $P_0 = (2, 3, 1)$ and $P_1 = (2, 1, 3)$, for which $\Delta_0 = (\mathbf{r}_{21}, \mathbf{r}_{32}, \mathbf{r}_{13})$ and $\Delta_1 = (\mathbf{r}_{21}, -\mathbf{r}_{12}, \mathbf{0})$. Applying condition (A2) gives $\mathbf{r}_{12} \cdot \mathbf{r}_{31} > 0$ or $\theta_{213} < 90°$. But since the exchange must be stable with respect to all three pair exchanges, we find that *a three-particle reference point is maximal in the high-temperature limit iff the triangle is acute.*

One can make some progress for more than three particles. Let us examine whether the same triplet exchange ever passes closer to a pair permutation involving a fourth atom. That is, consider the same even permutation $P_0 = (2, 3, 1, 4)$, but take the odd permutation $P_1 = (4, 2, 3, 1)$. Then $\Delta_0 = (\mathbf{r}_{21}, \mathbf{r}_{32}, \mathbf{r}_{13}, \mathbf{0})$ and $\Delta_1 = (\mathbf{r}_{41}, \mathbf{0}, \mathbf{0}, \mathbf{r}_{14})$. Applying condition (A2) gives $\|\mathbf{r}_{14} - \mathbf{r}_{12}/2\| < r_{12}/4$. This is an equation for a circle lying in half of the side of the triangle. Considering the other pair exchanges and the inverse triplet exchange P_0^{-1} will lead to five other circles. Consideration of the odd quadruple exchange does not lead to any new restrictions on the reference point. Sufficient (and I believe necessary) conditions that the point $P_0 R$ be connected to R is that no other particles lie inside the regions bounded by the six circles placed along the sides of the triangle and that the triangle be acute. Computationally, I find that these conditions hold in the high-temperature limit, but that nonacute exchanges are also possible at lower temperatures.

APPENDIX B. MAXIMAL NODES AND CLUSTERS

Here I show that if the N particles form a single cluster under a set of allowable triple permutations $\{p_{ijk}\}$, then the nodal cells are maximal. Let me review the definitions.

1. The reference point R_0 and the inverse temperature β are fixed.
2. A path $R(\lambda)$ is called allowable if the density matrix remains positive throughout the path

$$\rho_F(R(\lambda), R_0; \beta) > 0 \tag{B1}$$

   where $0 < \lambda < 1$.
3. An allowable triple permutation p_{ijk} is one for which the straight-line path from R_0 to $p_{ijk} R_0$ is allowable:

$$R(\lambda) = R_0 + \lambda(p_{ijk} R_0 - R_0) \tag{B2}$$

4. If the permutation p_{ijk} is allowable, we say that the particles (i, j) are connected. Of course this means also that (i, k) and (k, j) are connected. Connectedness is a binary attribute.

5. We say that an N-particle system forms a single cluster if for any two particles, there exists a connected path between them.
6. We say that an N-particle system has maximal nodal cells if for any two even permutations P_1 and P_2 there exists an allowable path connecting $P_1 R_0$ with $P_2 R_0$.

The proof is by induction on the number M of allowable triangles. For $M=1$ it is clearly true, since if p_{123} is allowable, so is p_{123}^{-1}. Now suppose that a single cluster implies maximal nodal cells if M or fewer allowable permutations are given. Given a system with $M+1$ allowable permutations forming a single cluster, I must find an allowable path between any two even permutations. I will do this by removing one of the permutations. The selection of which one to remove is important, since the wrong choice can lead to several clusters. I assert that it is possible to find a permutation P' such that if it is removed the remaining set of permutations is either:

1. A connected cluster of N particles and M permutations. In this case I am finished.
2. A connected cluster with $N-1$ particles and M permutations and one isolated (nonconnected) particle.
3. A connected cluster with $N-2$ particles and M permutations and two isolated (nonconnected) particles.

That P' exists is proven by asserting the contrary. Suppose removal of a triangle disconnects $K>2$ particles. Then one of the resulting clusters must contain two or more particles which are connected by a permutation. Removal of that permutation will then disconnect fewer than K particles unless $K \leqslant 2$.

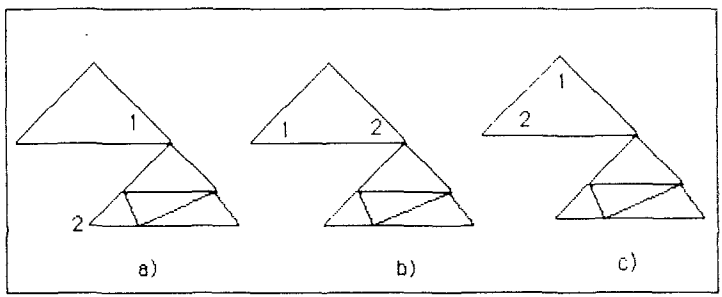

Fig. 9. Schematic of how one can move the labels (1, 2) from an arbitrary position (a) to the final positions in (c). The other nodes of the cluster are then unscrambled by the same (recursive) procedure on the subcluster obtained by removing the triangle containing (1, 2).

To finish the proof I must show how to construct an allowable path connecting any two even permutations P_1 and P_2 in cases 2 and 3 above. Case 2 is easy. Simply move the desired label onto the isolated particle with the connected path. Now no longer use P'. By assumption one can shuffle the remaining $(N-1, M)$ cluster. Case 3 is a bit more difficult, but a sequence of steps, illustrated in Fig. 9, allows the right labels to be placed on the two disconnected particles and then P' retired. Then one shuffles the remaining labels on the M cluster.

APPENDIX C. UNIQUENESS OF THE FIXED-NODE SOLUTION AND THE TILING PROPERTY OF THE REACH

Here I give the proof that replacing the initial conditions in all space for $\beta = 0$ is equivalent to fixing the boundary conditions on the reach of R_0. I need to show that inside this domain the exact fermion density matrix is the unique solution. The first point, that the exact fermion density matrix satisfies the boundary conditions, is obvious. Second, I need to show that the boundary conditions uniquely determine the solution.

First, suppose I have a function $\delta(R, t)$ satisfying the Bloch equation:

$$(\mathscr{H} + d/dt)\,\delta(R, t) = 0 \tag{C1}$$

in some space-time domain, vanishing at the edges of the domain and at time t_1:

$$\delta(R, t_1) = 0 \tag{C2}$$

Consider the following integral:

$$\int_{t_1}^{t_2} dt \int dR\, e^{2V_0 t}\delta(R, t)(\mathscr{H} + d/dt)\,\delta(R, t) = 0 \tag{C3}$$

where the spatial integral is over the domain and V_0 is a lower bound to the potential: $V_0 < V(R)$. The time integral of the term involving d/dt can be performed and using Green's identity and the boundary conditions on the surface of the domain for the kinetic energy term, we arrive at

$$\frac{e^{2V_0 t_2}}{2}\int dR\,\delta(R, t_2)^2 + \int_{t_1}^{t_2} dt\, e^{2V_0 t}\int dR\,[(V(R) - V_0)\,\delta(R, t)^2 + \lambda(\nabla\delta)^2] = 0 \tag{C4}$$

Note that each term is nonnegative, so that $\delta(R, t) = 0$ for all points in the domain and for $t_1 \leqslant t \leqslant t_2$.

We now follow the usual procedure of hypothesizing two solutions and showing that they must be the same. Let ρ_1 and ρ_2 be two solutions to the fixed-node problem and let $\delta = \rho_1 - \rho_2$. Then $\delta(R, t) = 0$ for $t_1 \leqslant t \leqslant t_2$. By taking t_2 to infinity and t_1 to zero, we conclude that the exact fermion density matrix is the unique solution.

Equation (C4) also shows that the reach has the tiling property. Suppose that it did not. Then there would exist a space-time domain with the density matrix nonzero inside and from which no paths exist to a reference point R_0 or any of its images PR_0 without crossing the nodes of the density matrix. But, such a domain cannot extend to $t = 0$, since in the classical limit one has the tiling property. Then this domain satisfies the conditions (C2) for some $t_1 > 0$ and must vanish completely inside the domain, contradicting the original assumption.

ACKNOWLEDGMENTS

I would like to thank Jerry Percus for many interesting conversations when I was first beginning to worry about fermion simulations, M. Caffarel for pointing out several of the references, G. Jacucci for discussions on the Voronoi problem in many dimensions, and E. L. Pollock and J. Theilhaber for discussions on fixed-node path integral Monte Carlo. I am supported by the National Science Foundation through grant NSF DMR88-08126, by the Department of Physics at the University of Illinois, and by the National Center for Supercomputing Applications. The computational aspects of this work used the CRAY-XMP at the National Center for Supercomputing Applications.

REFERENCES

1. D. M. Ceperley, G. V. Chester, and M. H. Kalos, *Phys. Rev. B* **16**:3081 (1977).
2. D. M. Ceperley and M. H. Kalos, in *Monte Carlo Methods in Statistical Physics*, K. Binder, ed. (Springer-Verlag, 1979).
3. D. M. Ceperley and B. J. Alder, *Phys. Rev. Lett.* **45**:566 (1980).
4. D. M. Ceperley, in *Recent Progress in Many-Body Theories*, J. Zabolitzky, ed. (Springer-Verlag, 1981).
5. E. L. Pollock and D. M. Ceperley, *Phys. Rev. B* **30**:2555 (1984).
6. D. M. Ceperley and B. J. Alder, *J. Chem. Phys.* **81**:5833 (1984).
7. D. M. Ceperley and E. L. Pollock, *Phys. Rev. Lett.* **56**:351 (1986).
8. J. P. Bouchaud and C. Lhuillier, *Europhys. Lett.* **3**:1273 (1987).
9. R. M. Panoff and J. Carlson, *Phys. Rev. Lett.* **62**:1130 (1989).
10. R. P. Feynamn and A. R. Hibbs, *Quantum Mechanics and Path Integrals* (McGraw-Hill, New York, 1965).
11. R. P. Feynman, *Statistical Mechanics* (Benjamin, 1972).
12. R. P. Feynman and M. Cohen, *Phys. Rev.* **102**:1189 (1956).

13. T. Muir, *A Treatise on the Theory of Determinants* (Dover, 1938).
14. D. J. Klein and H. M. Pickett, *J. Chem. Phys.* **64**:4811 (1976).
15. E. H. Lieb and D. C. Mattis, *Phys. Rev.* **125**:164 (1962).
16. J. B. Anderson, *J. Chem. Phys.* **63**:1499 (1975); **65**:4122 (1976).
17. W. L. McMillan, *Phys. Rev. A* **138**:442 (1965).
18. M. Caffarel and P. Claverie, *J. Chem. Phys.* **88**:1088 (1988).
19. P. Pechukas, *J. Chem. Phys.* **57**:5577 (1972).
20. O. Penrose and L. Onsager, *Phys. Rev.* **104**:576 (1987).
21. K. E. Schmidt and M. H. Kalos, in *Monte Carlo Methods in Statistical Physics II, Topics in Current Physics*, K. Binder, ed. (Springer-Verlag, 1984).
22. K. E. Schmidt, M. H. Kalos, M. A. Lee, and G. V. Chester, *Phys. Rev. Lett.* **45**:573 (1980).